

Poly((2,5-dialkoxy-*p*-phenylene)ethynylene-*p*-phenyleneethynylene)s and Their Model Compounds

Hong Li, Douglas R. Powell, Randy K. Hayashi, and Robert West*

Department of Chemistry, University of Wisconsin—Madison, 1101 University Avenue, Madison, Wisconsin 53706

Received June 20, 1997; Revised Manuscript Received November 12, 1997

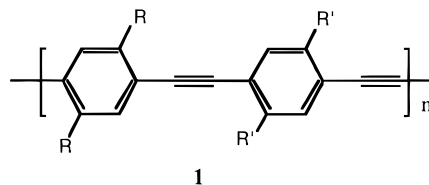
ABSTRACT: Poly((2,5-bis(*n*-hexyloxy)-*p*-phenylene)ethynylene-*p*-phenyleneethynylene) (**1a**), poly((2,5-bis(*n*-dodecyloxy)-*p*-phenylene)ethynylene-*p*-phenyleneethynylene) (**1b**), 1,4-diphenylethynylene-2,5-bis(*n*-hexyloxy)benzene (**2a**), and 1,4-diphenylethynylene-2,5-bis(*n*-dodecyloxy)benzene (**2b**) have been prepared by the Heck reaction. The X-ray crystal structures of **2a** and **2b** show that the overlap between aryl rings in neighboring molecules is small for **2a** but large for **2b**. **2a** and **2b** have similar electronic absorption spectra, and emission spectra in dilute solution, but the thin film emission of **2b** is red shifted about 40 nm, perhaps due to excimer cluster formation or aggregation. Likewise, polymers **1a** and **1b** have similar absorption spectra and emission spectra in solution, but in the solid state the emission of **1b** is significantly red shifted, also consistent with aggregation.

I. Introduction

The growing need for photoluminescent (PL) and electroluminescent (EL) devices, especially for the large-area light-emitting displays,¹ has stimulated fundamental materials research and organic synthesis. Several classes of organic polymers, poly(*p*-phenylene),² poly(*p*-phenylenevinylene),³ poly(phenyleneethynylene),⁴ and polythiophene⁵ have been found to be promising for the generation of light by means of electron and hole injection. Current research interests on EL polymers include tailoring of the spectral characteristics and the improvement of their processability and long-term stability. One of the most challenging problems is to optimize the radiative recombination efficiency and the carrier transport characteristics of the EL materials in order to achieve high quantum yields in photoluminescence and high-efficiency EL devices.⁶

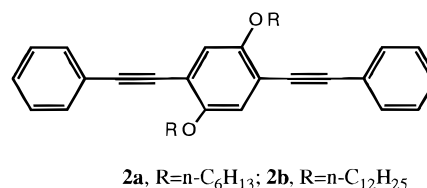
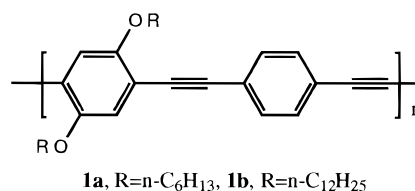
Excimer formation and fluorescence, initially identified in pyrene solution,⁷ are common to most aromatic hydrocarbons and their derivatives.⁸ The excimer, a sandwich dimer,⁹ is formed by the interaction of a ground state molecule with an excited molecule. The distance between sandwiched aromatic rings typically is within 3.3 Å.¹⁰ To form an excimer, the distance between the ground state aromatic rings should be less than 3.6 Å.¹¹ Excimer theory accounts well for the red shift of the fluorescence band in high concentration. The main chain of a poly(phenyleneethynylene) polymer is believed to have a planar and intrinsically straight "rigid rod" structure in the solid state.⁶ Thus excimer formation is expected in these polymers.

The first synthesis of poly(phenyleneethynylene) oligomers was reported in 1983.¹² The oligomerization was accomplished by heating cuprous acetylide with iodobenzene to a yellow-brown powder, which contained 10–12 phenyleneethynylene repeat units. More conveniently, a palladium-catalyzed polycondensation (the Heck coupling reaction) has been used to synthesize poly(phenyleneethynylenes).¹⁸ Le Moigne's group¹³ and Wrighton's group⁶ have reported the synthesis, structure ordering, and photoproperties of a series of polymers and oligomers with general structure **1**. The polymer structures were investigated by film or powder



X-ray diffraction. The relation between molecular structure and photoproperties, however, was not clear from these earlier studies.

In this paper, we report the synthesis and characterization of **1a**, **1b**, **2a**, and **2b** and the crystal structure of **2a** and **2b**, as the model compounds for polymers **1a** and **1b**. Because of the intense fluorescence of these materials, the photoproperties of **1a**, **1b**, **2a**, and **2b** have been studied in some detail.



II. Results and Discussion

Synthesis. 1,4-Diethynylbenzene was prepared by following a procedure described in the literature.¹⁴ 2,5-Diiodo-1,4-bis(*n*-hexyloxy)benzene and 2,5-diiodo-1,4-bis(*n*-dodecyloxy)benzene¹⁵ were synthesized by treating the corresponding 1,4-bis(*n*-alkyloxy)benzenes with I₂ and KIO₄ in acetic acid–water–sulfuric acid (90:7:3 by volume) solvent at 70 °C for 6 h. After recrystallization from ethanol, only diiodo- compounds were obtained.¹⁶ 2,5-Dibromo-1,4-bis(*n*-dodecyloxy)benzene was synthesized from 1,4-bis(*n*-dodecyloxy)benzene and Br₂ in CCl₄.¹⁷

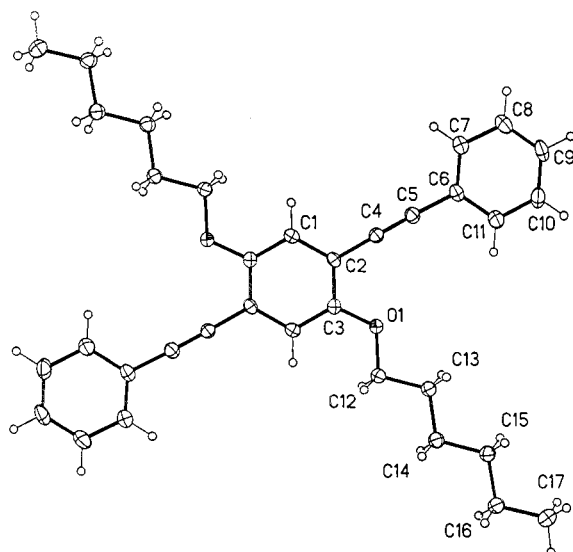
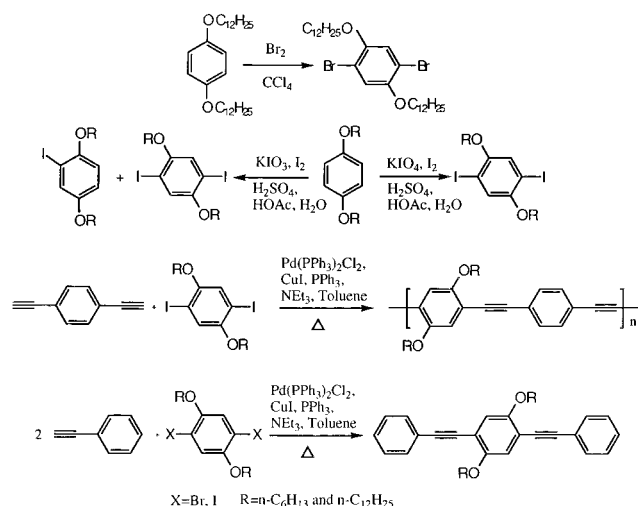


Figure 1. Crystal structure of **2a** with selected bond distances (Å) and angles (deg): C(2)–C(3) 1.412(2) Å, C(2)–C(4) 1.4369(14) Å, C(4)–C(5) 1.199(2) Å, C(13)–C(14) 1.525 Å, C(5)–C(4)–C(2) 178.47(12)°, C(4)–C(5)–C(6) 178.19(12)°, C(3)–O(1)–C(12) 117.65(8)°, O(1)–C(12)–C(13) 107.12(8)°.

Scheme 1



The polymers (**1a** and **1b**) and model compounds (**2a** and **2b**) were synthesized by a palladium-catalyzed cross-coupling reaction of diiodobenzene and acetylene derivatives, as shown in Scheme 1.¹⁸

X-ray Crystal Structures. The crystal structure of **2a** is shown in the thermal ellipsoid diagram of Figure 1, and a packing diagram of **2a** is shown in Figure 2. The hexyl side chains are extended in an all-*trans* conformation. The torsion angles for C1–C2–C6–C7 (4.8°) and C1–C2–C6–C11 (175.3°) show that the terminal phenyl rings are slightly tilted with respect to the central aryl ring. The central ring in one molecule is in close proximity to the side chain of a neighboring molecule. Although the overlap between aromatic rings in neighboring parallel molecules is small, the perpendicular distance (3.324 Å) between aryl rings and the shortest intermolecular contact distances C3–C12' (3.524 Å) and C3–O1' (3.509 Å) indicate that the van der Waals forces are fairly strong. A summary of the crystal data is given in Table 1.

Single crystals of **2b** were obtained by recrystallization from hexane. The structure of **2b** is shown in

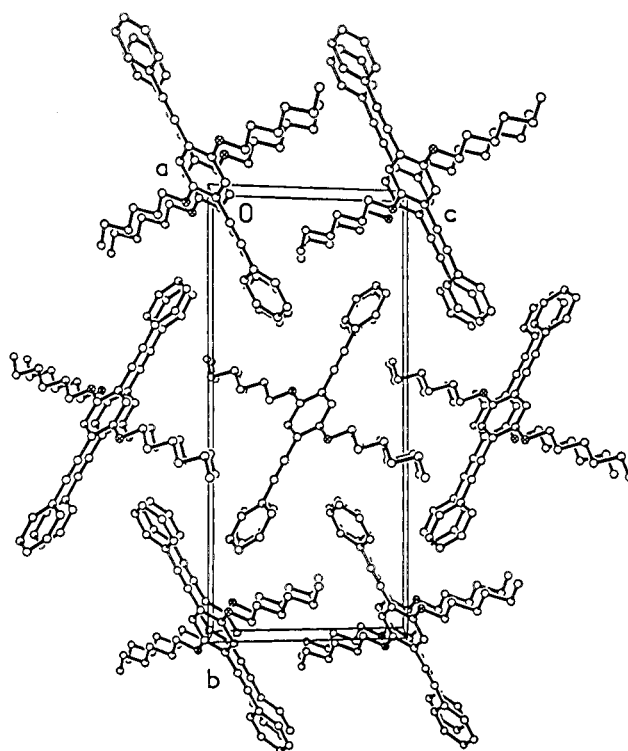


Figure 2. Packing diagram of **2a**.

Table 1. Summary of Crystal Data and Structure Refinement for 2a and 2b

compounds	2a	2b
empirical formula	C ₃₄ H ₃₈ O ₂	C ₄₆ H ₆₂ O ₂
crystal color	colorless	yellow
crystal size (mm)	0.40 × 0.15 × 0.15	0.46 × 0.22 × 0.04
crystal system	monoclinic	monoclinic
space group	<i>P</i> 2 ₁ / <i>c</i>	<i>P</i> 2 ₁ / <i>c</i>
<i>a</i> (Å)	6.1661(2)	25.0959(7)
<i>b</i> (Å)	22.9595(3)	5.0848(2)
<i>c</i> (Å)	10.5025(2)	16.0606(5)
α (deg)	90	90
β (deg)	106.923(2)	104.618
γ (deg)	90	90
volume (Å ³)	1422.46(6)	1983.11(11)
peaks to determine cell	4206	3963
θ range of cell peaks (deg)	3.0–25.0	3.0–25.0
temperature (K)	133(2)	133(2)
wavelength (Å)	0.71073	0.71073
<i>Z</i>	2	2
formula weight	478.64	646.96
density (g cm ⁻³)	1.118	1.083
absorption coefficient (mm ⁻¹)	0.067	0.064
<i>F</i> (000)	516	708
θ range for collection (deg)	1.77–28.29	1.68–28.20
<i>h</i>	–7 ≤ <i>h</i> ≤ 3	–32 ≤ <i>h</i> ≤ 31
<i>k</i>	–28 ≤ <i>k</i> ≤ 29	0 ≤ <i>k</i> ≤ 6
<i>l</i>	–5 ≤ <i>l</i> ≤ 13	0 ≤ <i>l</i> ≤ 20
standard peaks	133	108
no. of reflns collected	6155	10079
no. of indep reflns (<i>R</i> _{int})	2876 (0.0174)	4337 (0.0369)
goodness-of-fit on <i>F</i> ²	1.040	1.021
<i>R</i> (<i>F</i>), <i>wR</i> ₂ [<i>I</i> > 2σ(<i>I</i>)]	0.0366, 0.0896	<i>wR</i> ₂ = 0.1470
<i>R</i> (<i>F</i>), <i>wR</i> ₂ (all data)	0.0501, 0.0984	<i>R</i> ₁ = 0.0576
(Δρ) _{max,min} (e Å ⁻³)	0.928, 0.792	0.978, 0.734

Figure 3 and a packing diagram is displayed in Figure 4. Again, the side chain dodecyl groups are not coiled but are extended all-*trans*. The torsion angles of C2–C3–C6–C7 (0.3°) and C2–C3–C6–C11 (179.6°) indicate that the three aryl rings are all coplanar. The perpendicular distance (3.118 Å) between two central

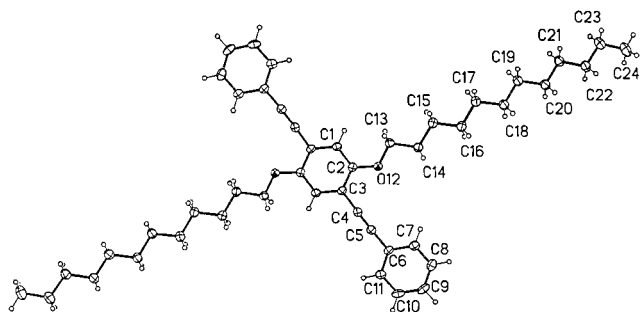


Figure 3. Crystal structure of **2b** with selected bond distances (Å) and angles (deg): C(2)–C(3) 1.411(2) Å, C(3)–C(4) 1.438(2) Å, C(4)–C(5) 1.205(2) Å, C(14)–C(15) 1.525 Å, C(5)–C(4)–C(3) 178.8(2), C(4)–C(5)–C(6) 176.8(2), C(2)–O(12)–C(13) 117.66(13), O(12)–C(13)–C(14) 107.18(14).

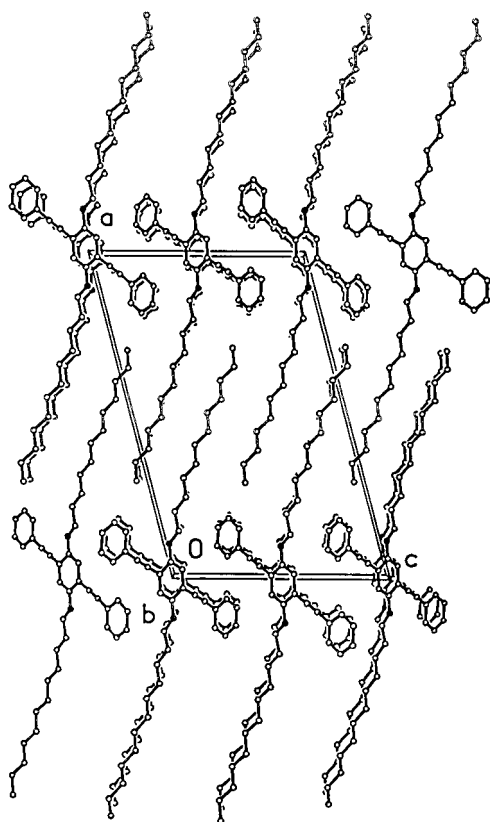


Figure 4. Packing diagram of **2b**.

aryl rings in neighboring molecules is shorter than that in **2a**. The shortest intermolecular contact distances C1–C4' (3.332 Å) and C2–C5' (3.354 Å) indicate very strong intermolecular interactions and large orbital overlap between aromatic rings in neighboring parallel molecules.

Characterization of Polymers. The weight average molecular weights of polymers **1a** (27 600) and **1b** (24 400) were measured by GPC. The molecular weights of polymers were highly dependent on the purity of monomers and the quality of the catalyst. Freshly recrystallized Pd(PPh₃)₂Cl₂ catalyst gave much higher molecular weights than catalyst which had been exposed to air. The solubility of the polymers depended on the nature of the side chains. **1a** was barely soluble in common organic solvents; less than 0.8 mg of **1a** could be dissolved in 1 L of THF. This polymer was slightly soluble in hot toluene. **1b**, however, proved to be soluble in THF, toluene, chloroform, benzene, and other solvents.

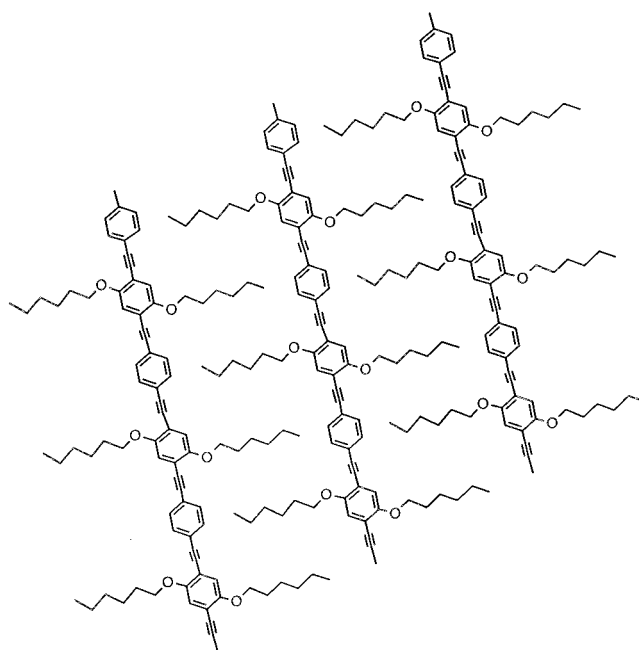


Figure 5. Proposed structures of **1a** and **1b** (strongly idealized).

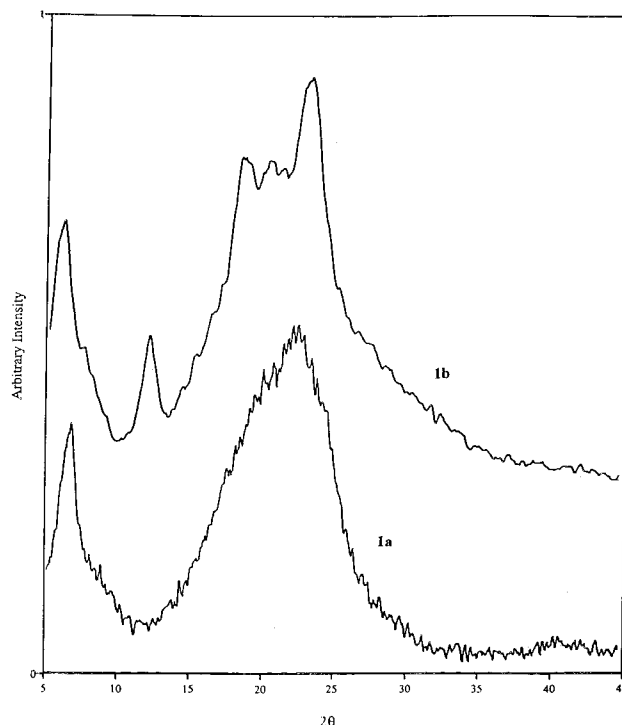


Figure 6. X-ray diffractogram of films **1a** and **1b**.

Solid State Structure. For polymers **1a** and **1b** with long main chains, we propose an idealized solid state structure shown in Figure 5, similar to the packing diagram of **2b** and the structure proposed by Le Moigne and his co-workers.¹³ In this proposed structure, the alkyl side chains of one molecule are inserted between the side chains of the neighboring molecules. The supramolecular structures of the polymers were investigated for thin films. The wide-angle X-ray diffraction (WAXD) pattern of the polymers at 25 °C are shown in Figure 6. The widths of the peaks indicate a low degree of crystallinity. The diffraction pattern of **1b** shows relatively intense peaks at 23.1, 21.2, 12.1, and 6.0°,

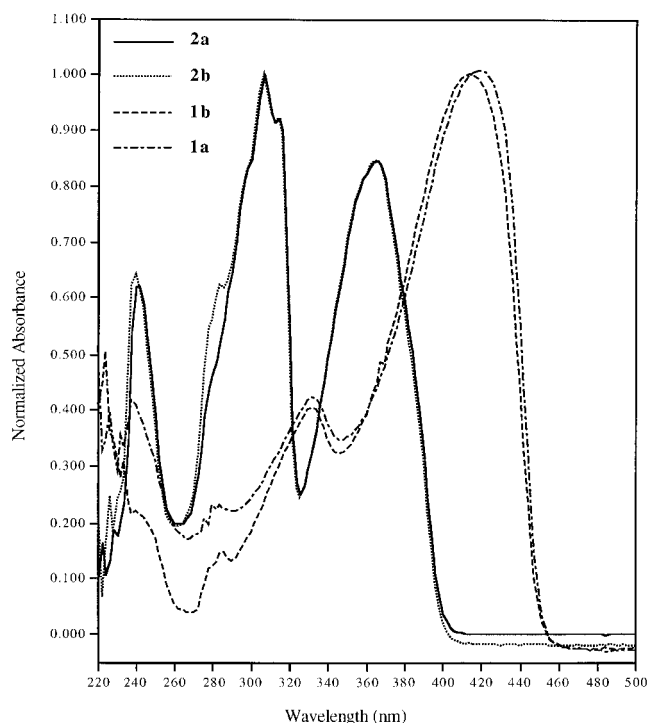


Figure 7. Absorption spectra of **1a**, **1b**, **2a**, and **2b** in THF.

which correspond to *d* spacings at 3.8, 4.2, 7.3, and 14.7 Å, respectively. The *d* spacings of 3.8 and 4.2 Å can be assigned as the distances of two aromatic ring planes between the rigid rod chains. Upon comparison of these results with the structure of **2b** (Figure 4), the perpendicular distance (3.118 Å) between two aryl planes of **2b** is about 0.7–1.1 Å shorter than that of polymer **1b**, suggesting that the main chain backbone of polymer **1b** may be slightly distorted from planarity. The *d* spacings of 14.7 Å in **1b** and 13.3 Å in **1a** represent the intermolecular distances between two main chains, as shown in Figure 5. Comparing the diffraction patterns of the two polymers, it is evident that **1b** is more ordered than **1a**.

The thermal stability was investigated by DSC from –50 to +420 °C. No phase transition was observed until polymers **1a** and **1b** decomposed at 370 and 400 °C, respectively.

Photoproperties. The absorption spectra of **1a**, **1b**, **2a**, and **2b** in THF solution are shown in Figure 7. The model compounds **2a** and **2b** have almost identical spectra, containing three absorption bands with peaks at 240, 306, and 366 nm. The 366 nm band is red shifted about 44 nm compared with that of (1,4-diphenylethynylene)benzene,¹⁹ due to the electron-donating effect of the alkoxy groups. For polymers **1a** and **1b**, two broad absorption bands with peaks at 332 and 414 nm were observed, which are characteristic for similar rigid rod polymers.¹⁷ The shapes and peaks of the absorption spectra are almost the same, independent of the nature of the side chains, for the two polymers both in solution and in the solid state. The absorption spectra of thin films of polymers **1a** and **1b** (Figure 8) showed maxima at 454 and 452 nm, respectively, red shifted about 40 nm compared to those of the same polymers in THF solution. This result indicates strong intermolecular interaction in the solid state.

The emission spectra in THF solution of **1a**, **1b**, **2a**, and **2b** are shown in Figure 9 (the concentrations used

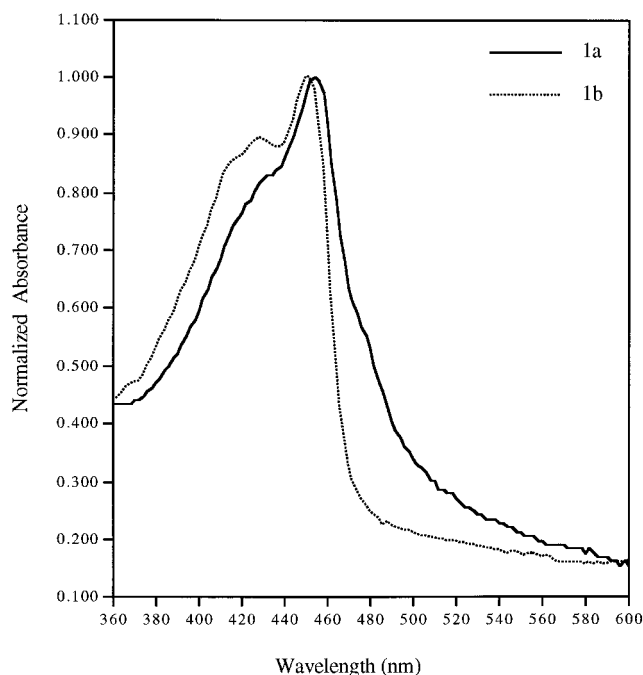


Figure 8. Solid state absorption spectra of **1a** and **1b**.

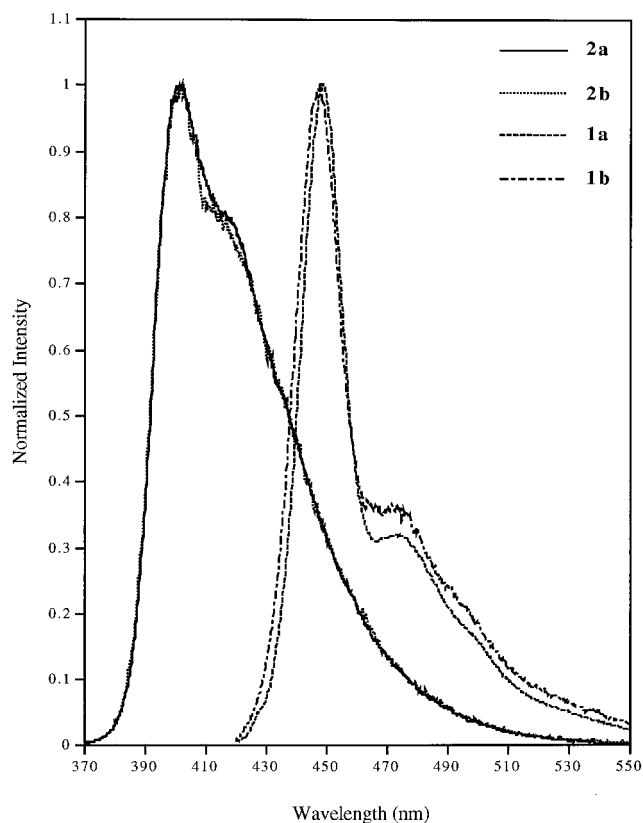


Figure 9. Emission spectra of **1a**, **1b**, **2a**, and **2b** in THF.

for measurement were about 10^{-7} mol/L for model compounds and 10^{-4} g/L for polymers). The spectra of model compounds **2a** and **2b** display an emission peak at 402 nm and a shoulder at 426 nm. When the concentration was increased from 10^{-7} to 10^{-2} mol/L, the shoulder at 426 nm became a peak (Figure 10). For the highly concentrated solution, the fluorescence was measured using the reflection method in a 0.1 mm cell. It is difficult to exclude self-absorption effects completely, but the crystal data for **2a** and **2b** show that

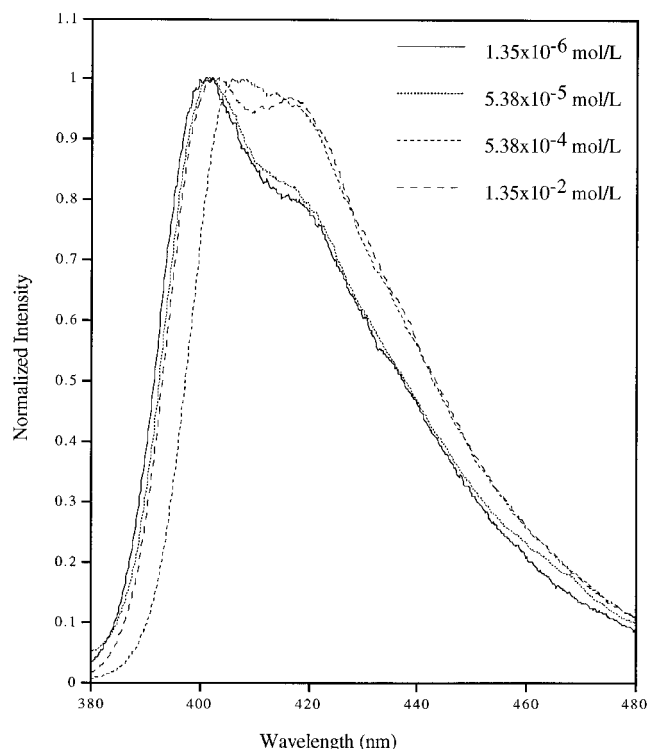


Figure 10. Concentration dependent fluorescence spectra of **2a** in THF solution.

the distances between aromatic rings are around 3.1–3.3 Å in these compounds, which strongly suggests that excimers can be formed in concentrated solution. Thus we suggest that the 426 nm shoulder is due to excimer formation rather than vibronic structure.

The emission spectra of polymers **1a** and **1b** show two peaks at 448 and 474 nm, red shifted about 46 nm compared to those of the model compounds. The fact that the polymer emission bands are much narrower than the absorption bands is consistent with emission from localized excited states, most likely after a migration of the excitons along the polymer main chain to segments that represent low-energy states. The concentration dependence of fluorescence of polymer **1b** was measured (Figure 11). The relative intensity of the band with a peak at 474 nm increased with concentration, similar to the behavior of **2b**. Thus we suggest that this band is also due to excimer formation.

The striking similarity of the electronic properties of **1a** and **1b**, or **2a** and **2b** in solution indicates that these molecular properties are predominantly governed by the rigid-rod conjugated backbone and are not influenced by the nature of the attached side chains.

The solid state emission spectra of **1a**, **1b**, **2a**, and **2b** were recorded as shown in Figure 12. The emission spectrum of **2a** showed highly structured peaks at 426, 437, and 462 nm, but the emission of **2b** is broad, showing only a peak at 475 nm. The different emission spectra in the solid state can be rationalized by the different crystal structures of **2a** and **2b**. Because the overlap of aromatic rings in neighboring molecules is small for **2a**, sandwich excimers could not be formed in the solid state. However, intermolecular interaction between an aromatic ring in one molecule and side chains of the other molecules may cause the solid emission band to be red shifted compared to that of the same compound in THF solution. In crystals of **2b**, the aromatic rings in neighboring molecules overlap each

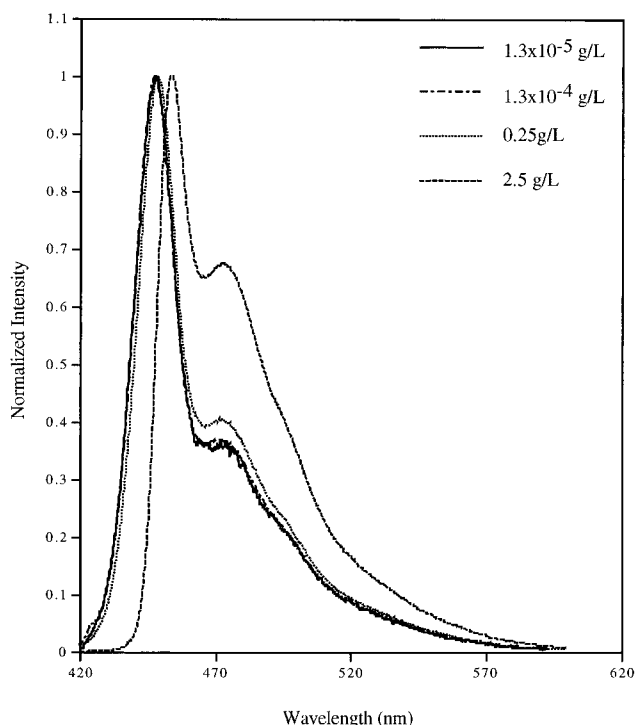


Figure 11. Concentration dependent fluorescence spectra of **1b** in THF solution.

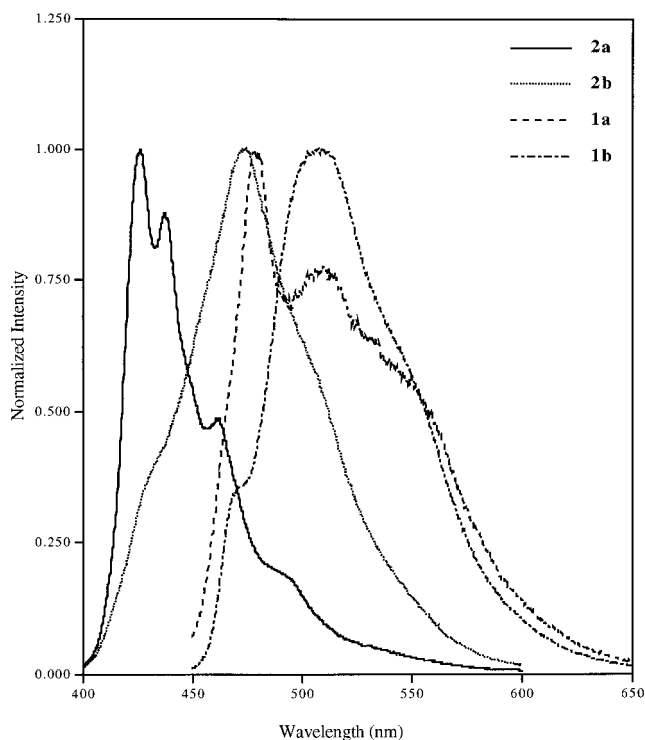


Figure 12. Film emission spectra of **1a**, **1b**, **2a**, and **2b**.

other with a distance of only 3.1 Å, indicating that aggregation may take place in the solid state and produce a further red shift of the emission band.²⁰ In the thin film emission spectra of polymers **1a** and **1b**, the emission spectra were broader and more red shifted. It seems likely that excimer clusters or aggregates are dominant in the emission spectra of the polymers.

The quantum yield for emission was measured in dilute THF solution in which UV absorbance is between 0.05 and 0.01. Quinine sulfate was used as the stan-

Table 2. Absorption Spectra, Fluorescence Spectra, and Quantum Yield^a of 1a, 1b, 2a, and 2b

name	absorption in THF (nm)	emission in THF (nm)	emission in solid state (nm)	Q in THF
1a	414, 332	449, 474	478, 511	1.00
1b (ε, m ² /g)	414 (58.7), 332 (23.8)	448, 474	507	1.00
2a (10 ³ ε, m ² /mol)	240 (2.52), 306 (4.05), 366 (3.43)	402, 426	426, 437, 462	0.93
2b (10 ³ ε, m ² /mol)	240 (2.68), 306 (4.16), 366 (3.52)	402, 426	475	0.95

^a Quantum yield of fluorescence refers to the measurements in THF solution.

dard. The excitation wavelength 366 nm was used, and the results are shown in Table 2. The quantum yield of samples in solution (Φ_s) relative to a reference sample of known quantum yield Φ_r was calculated by the following equation:²¹

$$\Phi_s = \Phi_r (A_r F_s / A_s F_r) (n_s^2 / n_r^2)$$

where A_s and A_r are the absorbances of the sample and reference solutions, respectively, at the same excitation wavelength, F_s and F_r are the corresponding relative integrated fluorescence intensities, n is the refractive index [refractive indices of pure THF ($n_s = 1.407$) and 1 N H₂SO₄ ($n_r = 1.339$) were used].²² Due to strong self-absorption and excimer formation of these compounds, the measured quantum yields are highly dependent on the concentration and excitation wavelength. Model compounds **2a** and **2b** and polymers **1a** and **1b** are intensely fluorescent materials. When the concentration is reduced to 10⁻⁷ mol/L, the quantum yields for these materials reach unity.²³

III. Conclusions

In summary, compounds **1a**, **1b**, **2a**, and **2b** have been synthesized by a palladium-catalyzed cross-coupling reaction. The X-ray single crystal results show that the aromatic rings of the neighboring molecules are overlapped in the structure of compound **2b**, but not in **2a**. The wide-angle X-ray diffraction pattern of the thin film indicates that polymer **1b** is more crystalline than polymer **1a**. The change of side chains from *n*-hexyl to *n*-dodecyl produces no striking difference in molecular photoproperties in dilute solution, but a red-shift in the solid state emission spectra was observed. Therefore, the nature of the side chain affects not only the solubility but also the solid state structures and photoproperties.

IV. Experimental Section

General Procedure. Proton and carbon nuclear magnetic resonance (¹H and ¹³C) spectra were recorded in deuterated solvent on a Bruker WP-300 (300 MHz for ¹H NMR, 75 MHz for ¹³C NMR). Chemical shifts are reported in ppm, relative to residual CHCl₃ (δ 7.24) and benzene (δ 7.14). The molecular weight was measured by gel permeation chromatography using a Waters Associates Model 6000A liquid chromatograph equipped with three American Polymer Standards Corp. Ultrastaygel columns in series with porosity indices of 10³, 10⁴, and 10⁵ Å, using freshly distilled THF as eluent. The polymer was detected with a Waters Model 440 ultraviolet absorbance detector at a wavelength of 254 nm, and the data were manipulated using a Waters Model 745 data module. Molecular weight was determined relative to polystyrene standards. Films for X-ray diffraction of polymers **1a** and **1b** were cast from a toluene slurry and dried under vacuum for 24 h at 110 °C. Measurement of the sample was done on a Nicolet I2/V diffractometer, with a Cu Kα beam. Absorption spectra were measured with a Hewlett Packard 8452A diode array spectrophotometer. Fluorescence emission and excitation spectra were recorded on a Hitachi Model F-4500 fluorescence spectrophotometer. DSC measurement was per-

formed with a 2910 TA instrument and a 2200 TA instrument controller using 4 mg of sample in a dry helium atmosphere (the samples were dried under vacuum at 110 °C for 24 h). All reactions were performed under N₂ or Ar atmosphere.

Synthesis of 2,5-Diiodo-1,4-bis(*n*-hexyloxy)benzene.

To a 250 mL three-necked flask equipped with condenser and magnetic stirrer were added 1,4-bis(hexyloxy)benzene (13.9 g, 0.05 mol), iodine (15.2 g, 0.06 mol), KIO₄ (13.8 g, 0.06 mol), acetic acid (90 mL), water (7 mL), and H₂SO₄ (3 mL). The reaction solution was stirred for 24 h at 70 °C and then cooled to room temperature. The mixture was poured into a 1 L beaker with 500 mL of water, and the resulting suspension was filtered to remove the solvent. The solid product was recrystallized from ethanol, yielding 22.4 g (85%) of product. ¹H NMR (300 MHz, C₆D₆): δ 0.90 (t, 6H), 1.25 (m, 12H), 1.53 (m, 4H), 3.30 (t, 4H), 7.06 (s, 2H). ¹³C NMR: δ 14.2, 22.9, 26.0, 29.3, 31.7, 69.9, 86.6, 122.9, 153.3.

A similar procedure was used to synthesize 2,5-diiodo-1,4-bis(*n*-dodecyloxy)benzene. ¹H NMR (300 MHz, C₆D₆): δ 0.92 (t, 6H), 1.30 (b, 40H), 1.55 (p, 4H), 3.38 (t, 4H), 6.95 (s, 2H). ¹³C NMR: δ 14.1, 22.7, 26.0, 29.2, 29.3, 29.4, 29.5, 29.6, 29.7, 31.9, 70.4, 86.32, 122.8, 152.9.

Synthesis of 2a. In a 250 mL three-necked flask with a magnetic stir bar were combined acetylbenzene (1.4 g, 13.7 mmol), 2,5-diiodo-1,4-bis(hexyloxy)benzene (3.67 g, 6.92 mmol), a catalytic amount of CuI, PPh₃, Pd(PPh₃)₂Cl₂, NEt₃ (20 mL), and benzene (100 mL). The mixture was stirred for 24 h at room temperature. The salts were filtered, and the solvent was removed under vacuum. The residue was recrystallized from hexane, giving 3.0 g (91%) of **2a**, mp 114–115 °C. ¹H NMR (300 MHz, CDCl₃): δ 0.80 (t, 6H), 1.35 (m, 8H), 1.57 (m, 4H), 1.86 (p, 4H), 4.05 (t, 4H), 7.02 (s, 2H), 7.35 (m, 6H), 7.57 (m, 4H). ¹³C NMR: δ 14.02, 22.62, 25.73, 29.31, 31.59, 69.61, 85.97, 94.81, 113.97, 116.94, 123.47, 128.21, 128.28, 131.55, 153.64. MS: *m/e* (rel intensity) 478 (M⁺, 100), 407 (8.55), 394 (13.9), 323 (15.3), 310 (58.9), 281 (17.1), 253 (10.1), 252 (13.0), 43 (19.7).

Synthesis of 2b. To a 250 mL three-necked flask with a magnetic stir bar were added acetylbenzene (1.6 g, 15.7 mmol), 2,5-dibromo-1,4-bis(*n*-dodecyloxy)benzene (4.6 g, 7.61 mmol), a catalytic amount of CuI, PPh₃, Pd(PPh₃)₂Cl₂, NEt₃ (20 mL), and toluene (100 mL). The mixture was stirred for 24 h, and no salts were observed. The mixture was then heated at 115 °C for 10 h. After cooling to room temperature, the salts were filtered and the solvent was removed under vacuum. The resulting mixture was column chromatographed on silica gel, eluting with CH₂Cl₂/hexane (1:9 by volume) solvent. The last component was recrystallized from hexane, giving 3.7 g (76%) of **2b**, mp 80–81 °C. ¹H NMR (300 MHz, CDCl₃): δ 0.80 (t, 6H), 1.30 (b, 32H), 1.57 (p, 4H), 1.86 (p, 4H), 4.03 (t, 4H), 7.00 (s, 2H), 7.33 (m, 6H), 7.53 (m, 4H). ¹³C NMR: δ 14.11, 22.69, 26.11, 29.36, 29.41, 29.45, 29.63, 29.67, 29.70, 31.92, 69.73, 86.00, 94.82, 114.10, 117.11, 123.53, 128.21, 128.28, 131.58, 153.70. MS: *m/e* (rel intensity) 646 (M⁺, 100), 626 (10.7), 478 (9.75), 368 (12.7), 310 (23.0), 255 (12.3), 236 (22.3), 97 (13.0), 83 (12.5).

Synthesis of Polymer 1a. To a 250 mL three-necked flask equipped with condenser and magnetic stir bar were added 1,4-diethynylbenzene (0.951 g, 7.55 mmol), 2,5-diiodo-1,4-bis(*n*-hexyloxy)benzene (4.00 g, 7.55 mmol), NEt₃ (10 mL), toluene (100 mL), and a catalytic amount of CuI, Pd(PPh₃)₂Cl₂, and PPh₃. The mixture was stirred for 24 h at room temperature, then warmed to 40 °C for 24 h, and refluxed 24 h. After the reaction mixture was cooled to room temperature, the precipitate was removed by filtration, and the solvent was pumped

off. The residue was washed with water and then extracted with toluene at 115 °C for 24 h, and the resulting mixture was filtered. The extraction was repeated a second time. The solution was poured into a large amount of 2-propanol. The precipitate was collected, giving 2.4 g (75%) of polymer **1a**: $M_n = 15\,400$, $x_n = 37$ by ^1H NMR. ^1H NMR (CDCl_3 , ppm): δ , 0.87 (t, 6H), 1.35 (m, 4H), 1.55 (m, 8H), 1.85 (m, 4H), 4.00 (m, 4H), 7.00 (m, 2H), 7.50 (m, 4H).

Synthesis of Polymer 1b. 1,4-Diethynylbenzene (0.0875 g, 0.694 mmol), 2,5-diiodo-1,4-bis(*n*-dodecyloxy)benzene (0.485 g, 0.694 mmol), NEt_3 (5 mL), toluene (50 mL), a catalytic amount of CuI , $\text{Pd}(\text{PPh}_3)_2\text{Cl}_2$, and PPh_3 were added into a 100 mL three-necked flask equipped with condenser and magnetic stir bar. The mixture was stirred for 24 h at room temperature, warmed to 40 °C for 24 h, and refluxed for 24 h. After the reaction mixture was cooled to room temperature, the salts were filtered, and the solvent was removed under vacuum. The resulting solid was column chromatographed on silica gel, eluting with THF to remove catalysts. The first component was collected and precipitated by dropping the solution into 200 mL of 2-propanol and dried at 120 °C under vacuum, giving 0.34 g (85%) of polymer **1b**: $M_n = 14\,600$, $x_n = 24$ by ^1H NMR. ^1H NMR (CDCl_3 , ppm): δ 0.86 (6H, t), 1.1–1.6 (36 H, br), 1.8 (6H, m), 4.0 (4H, br), 6.8–7.35 (2H, m), 7.5 (4H, br). ^{13}C NMR: δ 14.16, 22.73, 26.09, 29.35, 29.39, 29.45, 29.65, 29.69, 29.72, 31.95, 32.3, 69.60, 116.81, 131.44, 153.62.

Acknowledgment. We thank the U.S. Office of Naval Research for financial support and the NSF (grant CHE-9310428) for the purchase of the X-ray instrument and computers.

Supporting Information Available: For **2a** and **2b**, tables giving the structure determination summary, positional and thermal parameters, atomic coordinates, bond distances and angles, and anisotropic displacement factors and structure diagrams (24 pages). Ordering and accessing information is given on any current masthead page.

References and Notes

- (1) Kido, J.; Hayase, H.; Hongawa, K.; Nagai, K.; Okuyama, K. *Appl. Phys. Lett.* **1994**, *65*, 2124.
- (2) Grem, G.; Leditzky, G.; Ullrich, B.; Leising, G. *Adv. Mater.* **1992**, *4*, 36.
- (3) (a) Burroughes, J. H.; Bradley, D. D. C.; Brown, A. R.; Marks, R. N.; Mackay, K.; Friend, R. H.; Burns, P. L.; Holmes, A. B. *Nature* **1990**, *347*, 539. (b) Braun, D.; Heeger, A. J.; Kroemer, H. *J. Electron. Mater.* **1991**, *20*, 945.
- (4) (a) Rutherford, D. R.; Stille, J. K.; Elliott, C. M.; Reichert, V. R. *Macromolecules* **1992**, *25*, 2294. (b) Sasabe, H.; Wada, T.; Hosoda, H.; Ohkawa, H.; Yamada, A.; Garito, A. F. *Mol. Cryst. Liq. Cryst.* **1990**, *189*, 155.
- (5) (a) Ohmori, Y.; Uchida, M.; Muro, K.; Yoshino, K. *Jpn. J. Appl. Phys.* **1991**, *30*, 11938. (b) Braun, D.; Gustafsson, G.; McBranch, D.; Heeger, A. J. *J. Appl. Phys.* **1992**, *72*, 564. (c) Greenham, N. C.; Brown, A. R.; Bradley, D. D. C.; Friend, R. H. *Synth. Met.* **1993**, *55–57*, 4143.
- (6) (a) Weder, C.; Wrighton, M. S. *Macromolecules* **1996**, *29*, 5157. (b) Ofer, D.; Swager, T. M.; Wrighton, M. S. *Chem. Mater.* **1995**, *7*, 418.
- (7) Förster, T.; Kasper, K.; Z. *Phys. Chem. (N. F.)* **1954**, *1*, 275.
- (8) Birks, J. B. *Acta. Phys. Polon.* **1964**, *26*, 367.
- (9) (a) Chandross, E. A.; Dempster, C. J. *J. Am. Chem. Soc.* **1970**, *92*, 704. (b) Chandross, E. A.; Dempster, C. J. *J. Am. Chem. Soc.* **1970**, *92*, 3586. (c) Chandra, A. K.; Lim, E. C. *J. Chem. Phys.* **1968**, *49*, 5066.
- (10) Sadygov, R. G.; Lim, E. C. *Chem. Phys. Lett.* **1994**, *225*, 441.
- (11) Birks, J. B. *Photophysics of Aromatic Molecules*; John Wiley & Sons Ltd.: London and Colchester, 1970.
- (12) Lakmikantham, M. V.; Vartikar, J.; Kwan, Y. J.; Cava, M. P.; Huang, W. S.; MacDiarmid, A. *Polym. Prepr. (Am. Chem. Soc., Div. Polym. Chem.)* **1983**, *24*, 75.
- (13) (a) Moroni, M.; Le Moigne, J.; Pham, T. A.; Bigot, J. Y. *Macromolecules* **1997**, *30*, 1964. (b) Wautelet, P.; Moroni, M.; Oswald, L.; Le Moigne, J.; Pham, T. A.; Bigot, J. Y. *Macromolecules* **1996**, *29*, 446.
- (14) (a) Takahashi, S.; Kuroyama, Y.; Sonogashira, K.; Hagihara, N. *Synthesis* **1980**, 627. (b) Hay, A. S. *J. Org. Chem.* **1960**, *25*, 637. (c) Sciebbzehrnl, F.; Nuyken, O. *Macromol. Chem.* **1988**, *189*, 541.
- (15) (a) Bao, Z.; Chen, Y.; Cai, R.; Yu, L. *Macromolecules* **1993**, *26*, 5281. (b) Bao, Z.; Chen, Y.; Cai, R.; Yu, L. *Polym. Prepr. (Am. Chem. Soc., Div. Polym. Chem.)* **1993**, *34*, 749.
- (16) Swager, T. M.; Gil, C. T.; Wrighton, M. S. *J. Phys. Chem.* **1995**, *99*, 4886. These workers recommend the use of KIO_3 instead of KIO_4 ; however, when we used KIO_3 , only a mixture of monoiodo and diiodo compounds was obtained, which was difficult to purify.
- (17) Moroni, M.; Le Moigne, J.; Luzzati, S. *Macromolecules* **1994**, *27*, 562.
- (18) Heck, R. F. *Palladium Reagents in Organic Synthesis*; Academic Press: New York, 1990.
- (19) (a) Gruzinskii, V. V.; Degtyarenko, K. M.; Kopylova, T. N.; Kuznetsov, A. L.; Novikov, A. N.; Sarycheva, T. A. *Zh. Prikl. Spektrosk.* **1987**, *46*, 52. (b) Nakatsuji, S.; Matsuda, K.; Uesugi, Y.; Nakashima, K.; Akiyama, S.; Fabian, W. *J. Chem. Soc., Perkin Trans. 1* **1992**, 755.
- (20) Saigusa, H.; Lim, E. C. *Acc. Chem. Res.* **1996**, *29*, 171.
- (21) Demas, J. N.; Crosby, G. A. *J. Phys. Chem.* **1971**, *75*, 991.
- (22) *CRC Handbook of Chemistry and Physics*, 77th ed.; CRC Press: Boca Raton, FL, 1996–1997; pp 8–77.
- (23) Fluorescence quantum yields approaching 1.0 for strongly fluorescent compounds in very dilute solutions are predated. See, for example: Jenekhe, S. A.; Osaheni, J. A. *Science* **1994**, *265*, 765.

MA970899D